

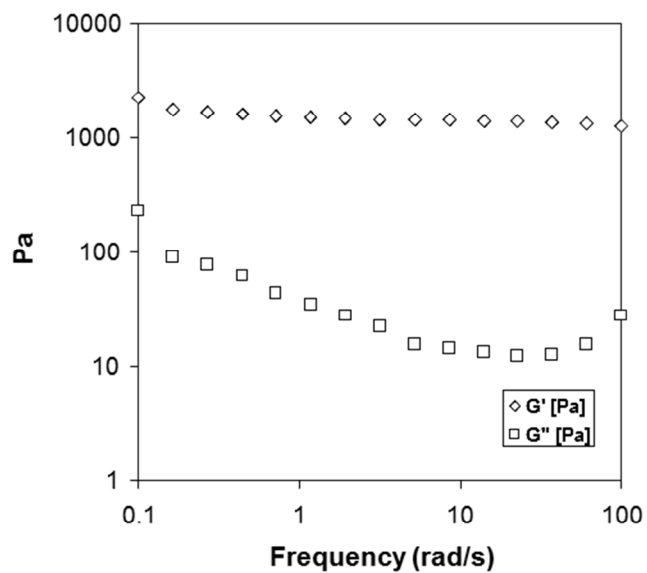
Supporting Information:

Table of Contents

Influence of hydrophobic face amino acids on the hydrogelation of β -hairpin peptide amphiphiles

<u>Content</u>	<u>Figure No.</u>
Dynamic frequency and strain sweep for M(Abu)	Fig. S1
Dynamic frequency and strain sweep for MAX1	Fig. S2
Dynamic frequency and strain sweep for M(Nva)	Fig. S3
Dynamic frequency and strain sweep for M(Nle)	Fig. S4
Dynamic frequency and strain sweep for M(Phe)	Fig. S5
Dynamic frequency and strain sweep for M(Ile)	Fig. S6
SANS data for M(Nva)	Fig. S7
SANS data for M(Nle)	Fig. S8
SANS data for M(Phe)	Fig. S9
SANS Data for M(Ile)	Fig. S10
RP-HPLC and ESI-MS of M(Abu)	Fig. S11
RP-HPLC and ESI-MS of MAX1	Fig. S12
RP-HPLC and ESI-MS of M(Nva)	Fig. S13
RP-HPLC and ESI-MS of M(Nle)	Fig. S14
RP-HPLC and ESI-MS of M(Phe)	Fig. S15
RP-HPLC and ESI-MS of M(Ile)	Fig. S16

A. Dynamic Frequency Sweep



B. Dynamic Strain Sweep

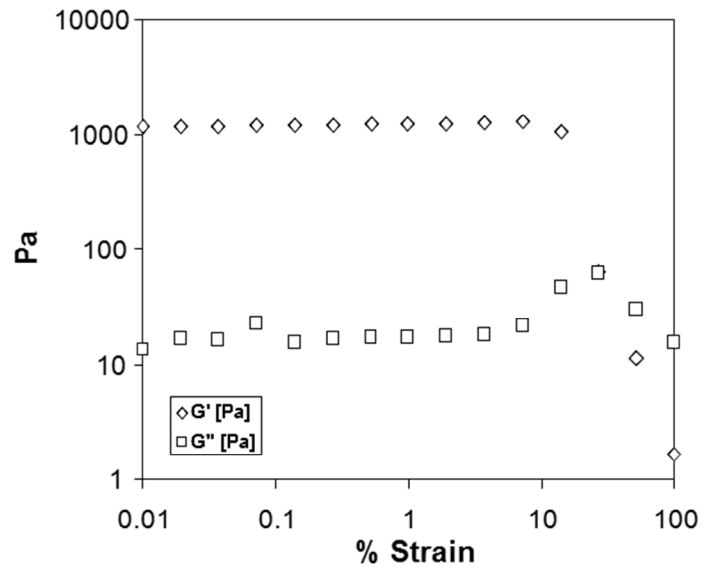


Figure S1: (A) Dynamic frequency and (B) strain sweep of 1wt% M(Abu) gels at 80°C in 125 mM borate, 10 mM NaCl, pH 9 buffer.

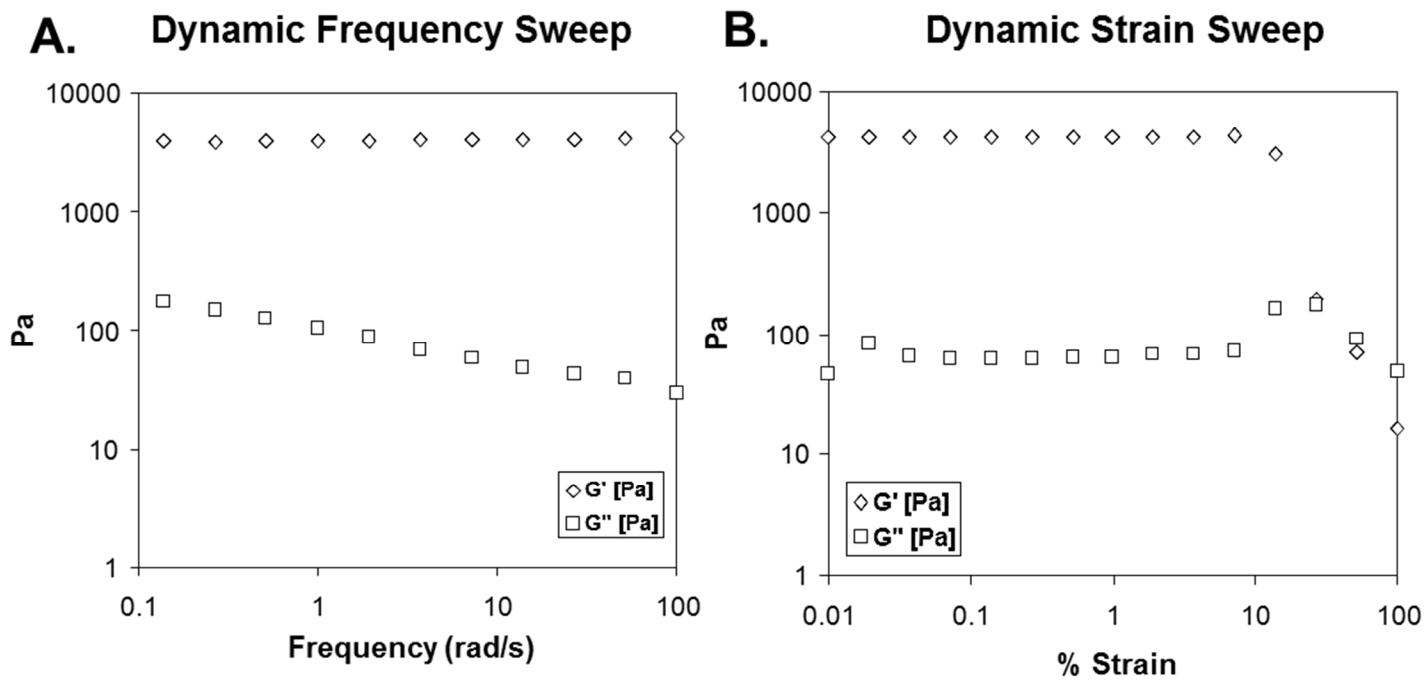
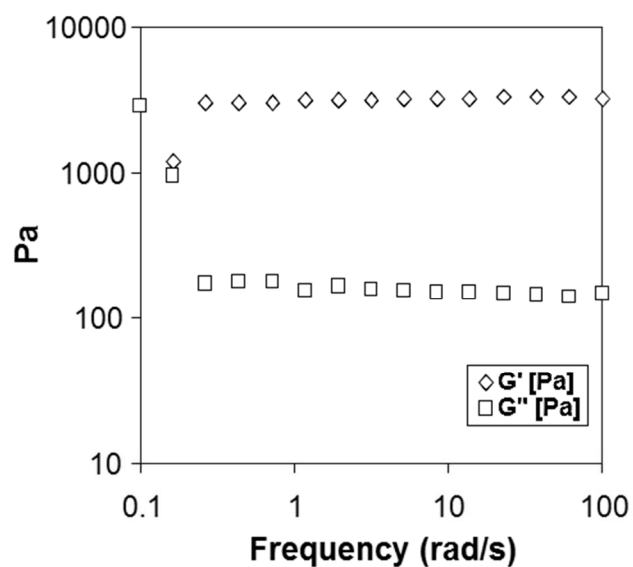


Figure S2: (A) Dynamic frequency and (B) strain sweep of 1wt% MAX1 gels at 50°C in 125 mM borate, 10 mM NaCl, pH 9 buffer.

A. Dynamic Frequency Sweep



B. Dynamic Strain Sweep

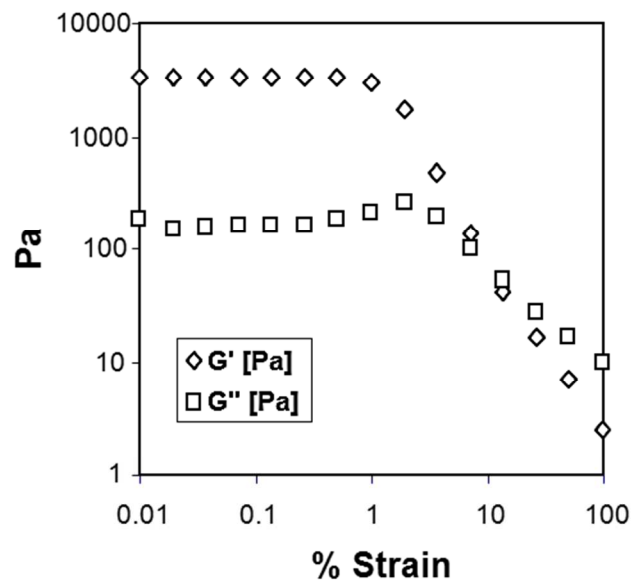
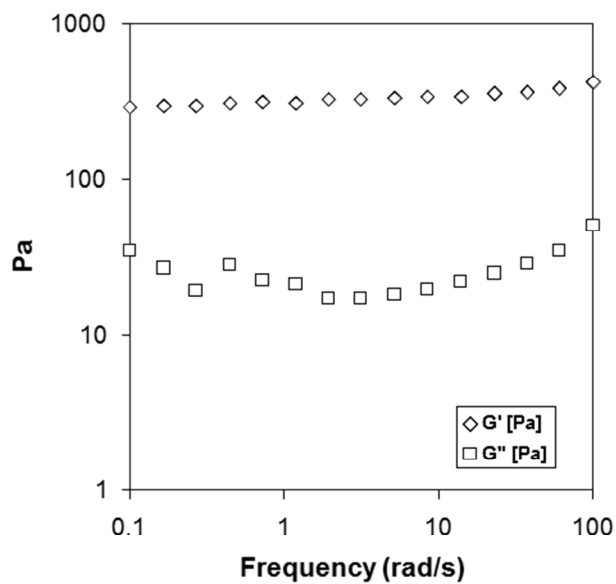


Figure S3: (A) Dynamic frequency and (B) strain sweep of 1wt% M(Nva) gels at 50°C in 125 mM borate, 10 mM NaCl, pH 9 buffer.

A. Dynamic Frequency Sweep



B. Dynamic Strain Sweep

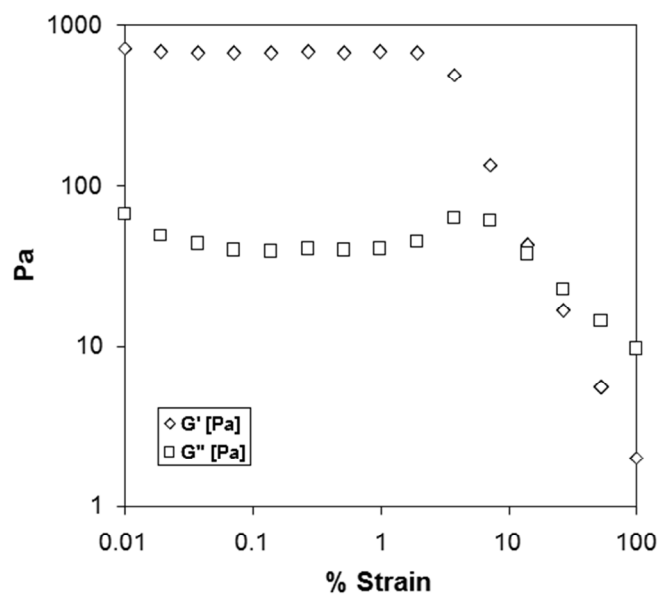


Figure S4: (A) Dynamic frequency and (B) strain sweep of 1wt% M(Nle) gels at 50°C in 125 mM borate, 10 mM NaCl, pH 9 buffer

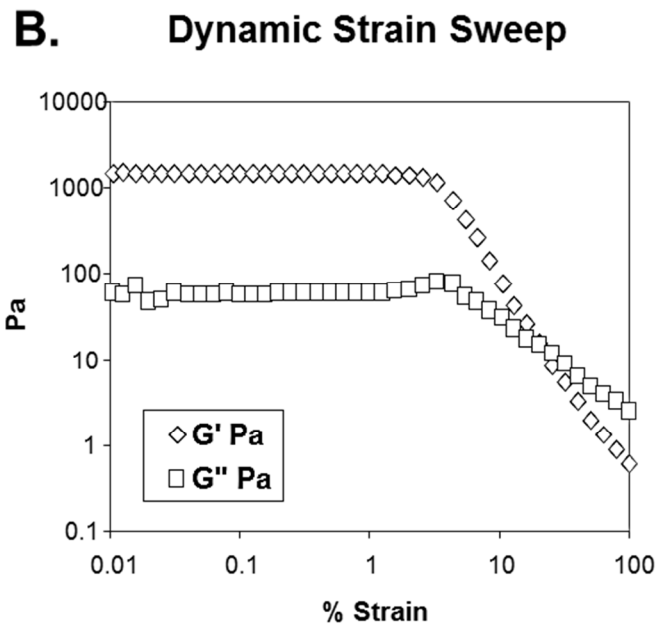
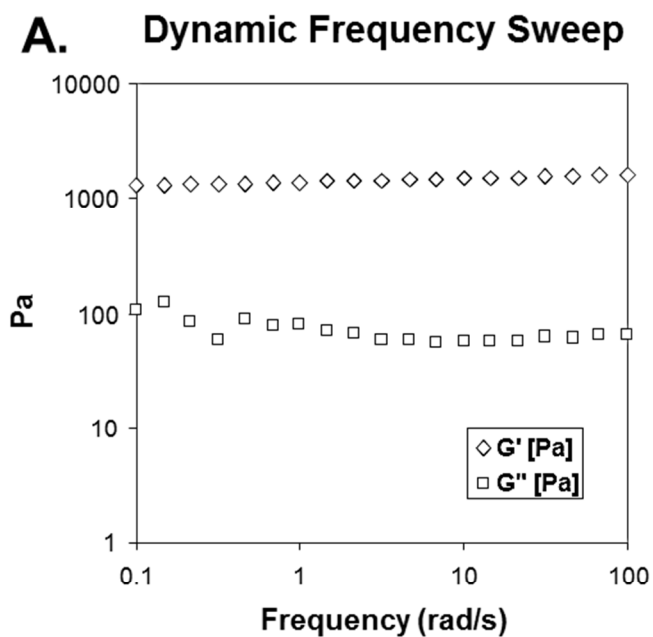


Figure S5: (A) Dynamic frequency and (B) strain sweep of 1wt% M(Phe) gels at 50°C in 125 mM borate, 10 mM NaCl, pH 9 buffer

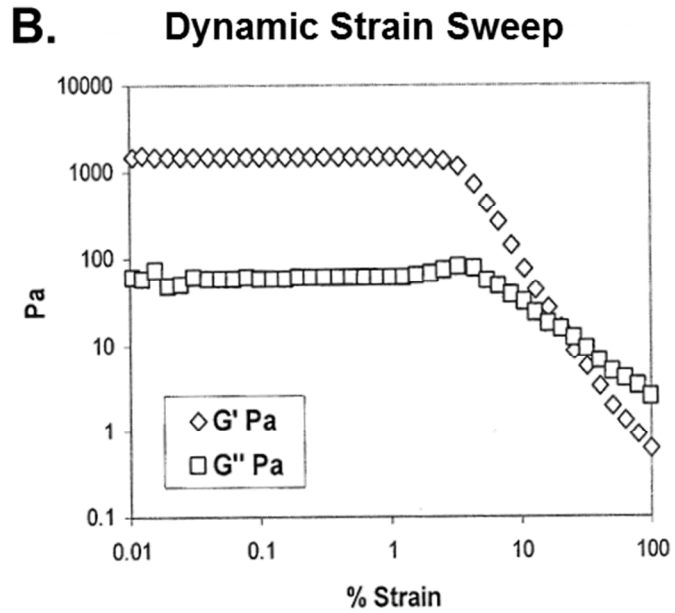
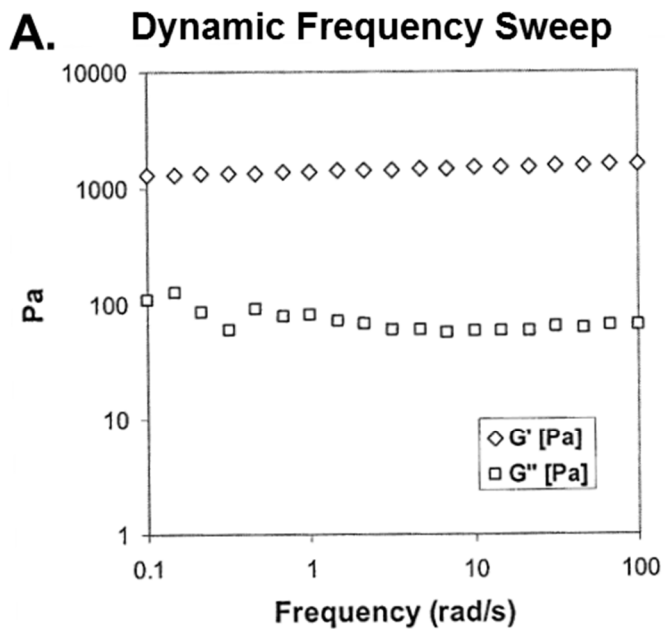


Figure S6: (A) Dynamic frequency and (B) strain sweep of 1wt% M(Ile) gels at 50°C in 125 mM borate, 10 mM NaCl, pH 9 buffer

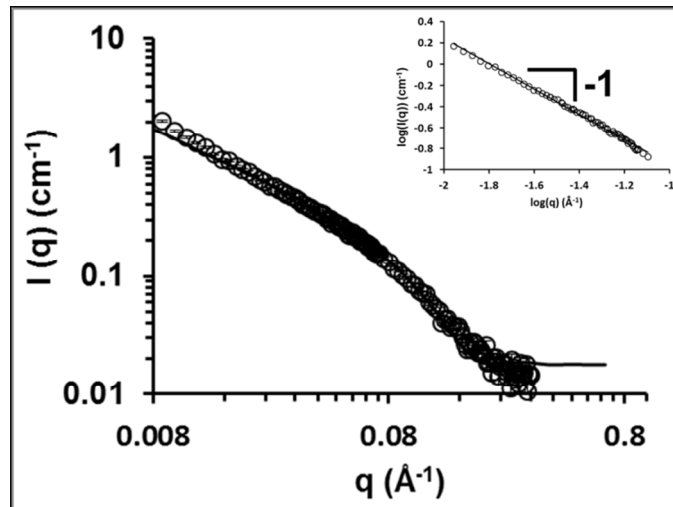


Figure S7: SANS analysis of M(Nva), with data fit using a cylindrical form factor. Inset shows a slope of approximately -1 for $\log I(q)$ versus $\log q$.

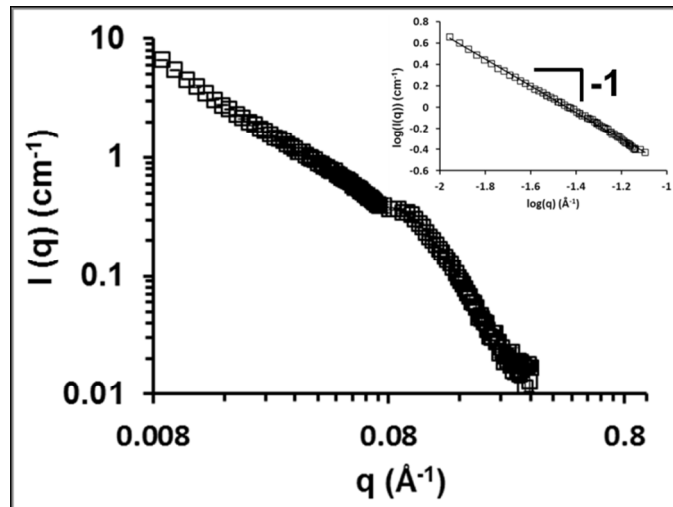


Figure S8: SANS analysis of M(Nle). Inset shows a slope of approximately -1 for $\log I(q)$ versus $\log q$.

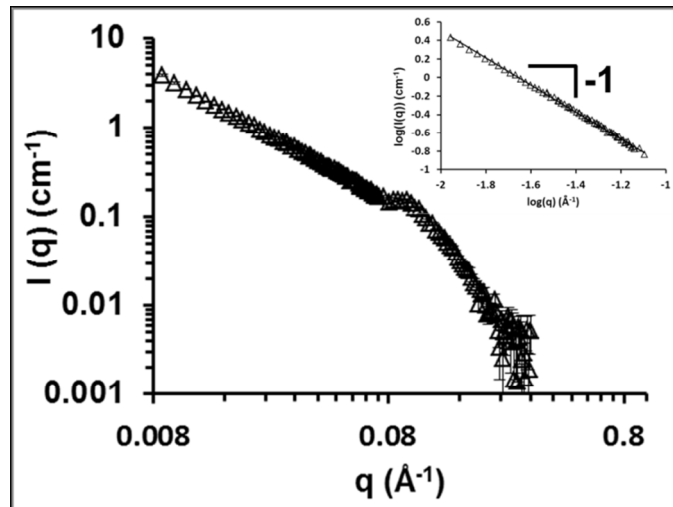


Figure S9: SANS analysis of M(Phe). Inset shows a slope of approximately -1 for $\log I(q)$ versus $\log q$.

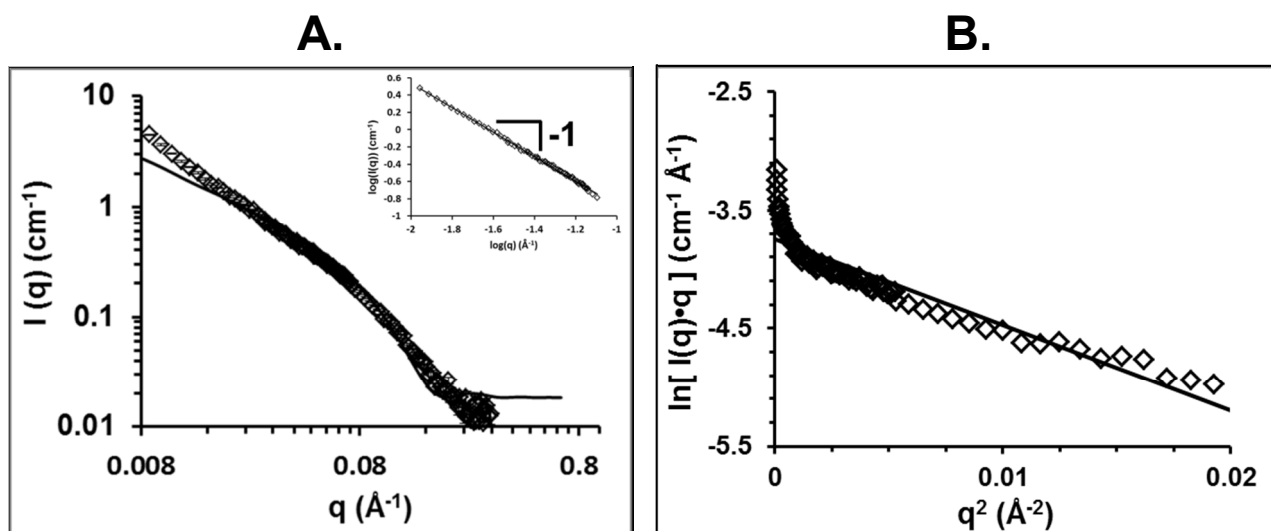


Figure S10: (A) SANS analysis of M(Ile), with data fit using a cylindrical form factor. Inset shows a slope of approximately -1 for $\log I(q)$ versus $\log q$. (B) SANS data for M(Ile) plotted as $\ln[I(q) \cdot q]$ vs q^2 . A linear fit was applied to the data in the low q regime to calculate fibril cross-sectional diameter using a modified Guinier analysis.

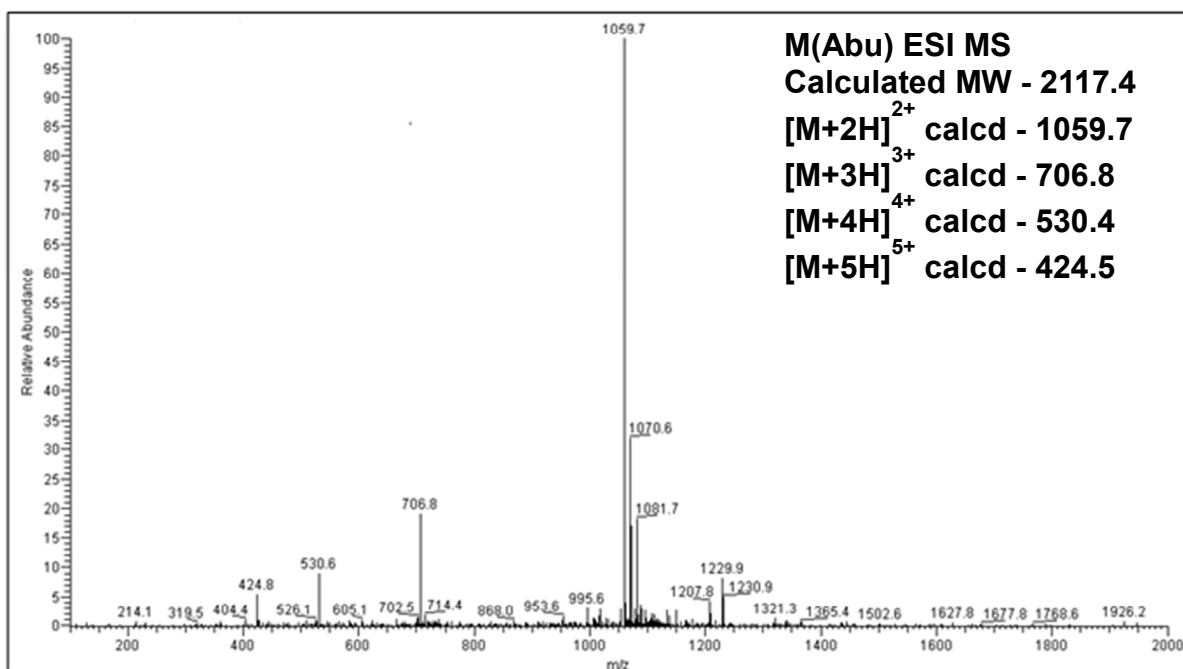
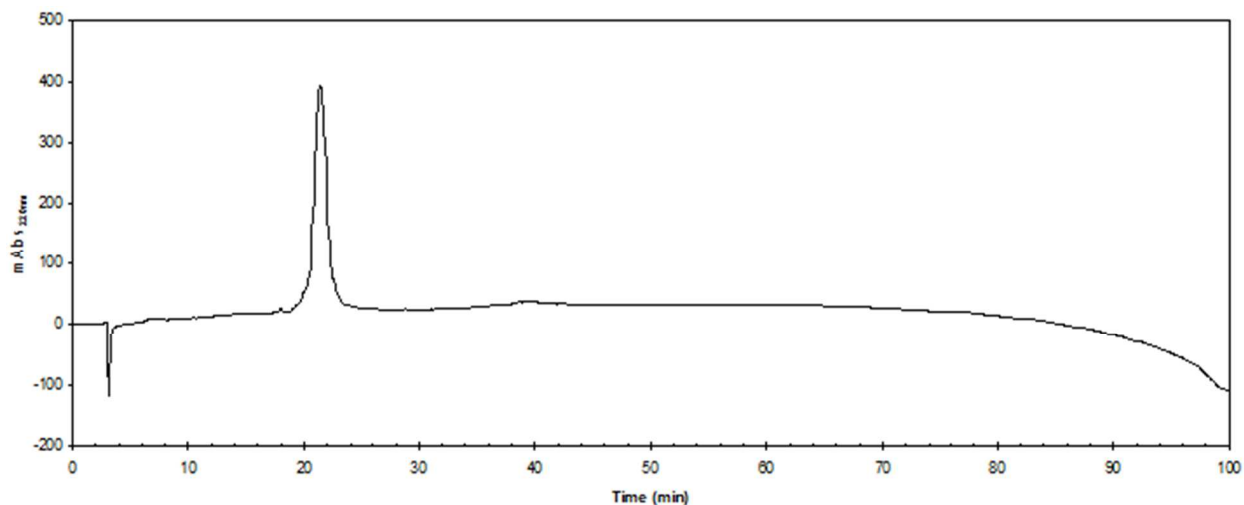


Figure S11: M(Abu) – Analytical HPLC (Vydac C18) 0-100% B; 100 min; 20°C.

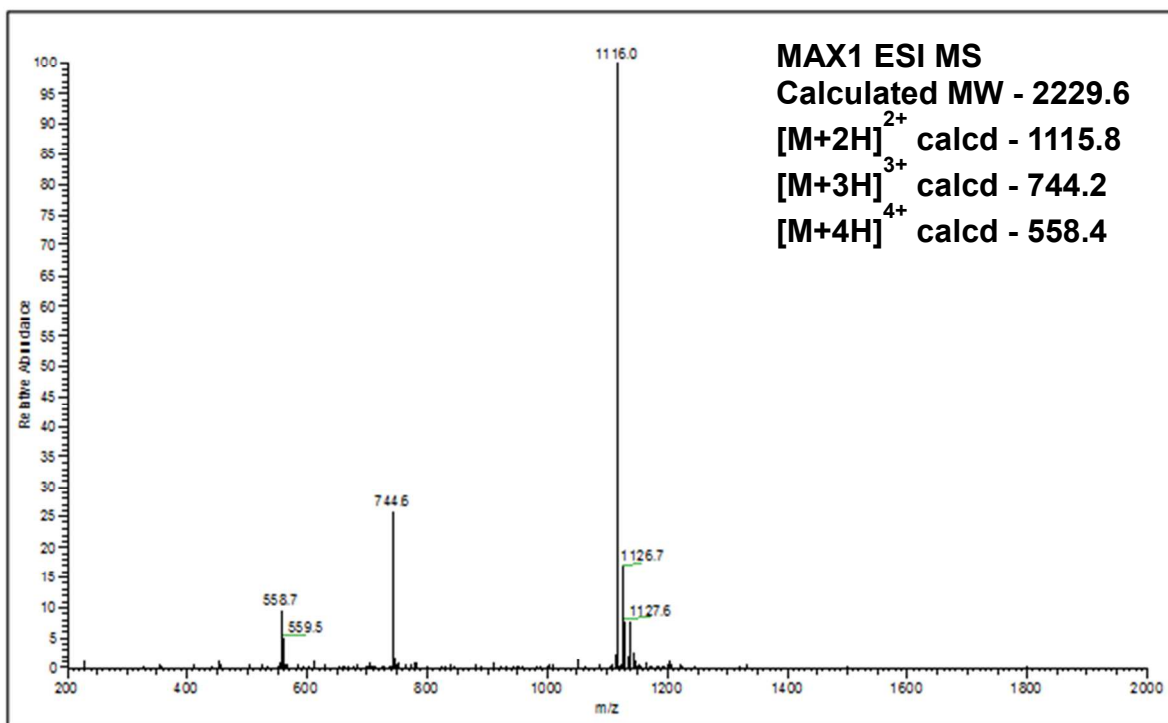
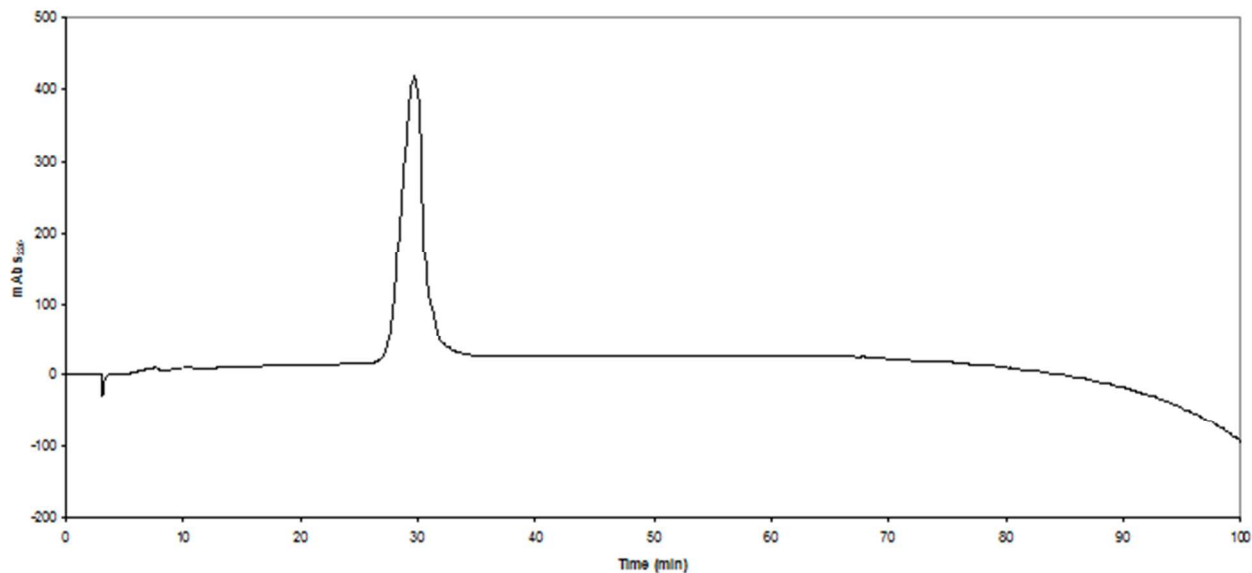


Figure S12: MAX1 – Analytical HPLC (Vydac C18) 0-100% B; 100 min; 20°C.

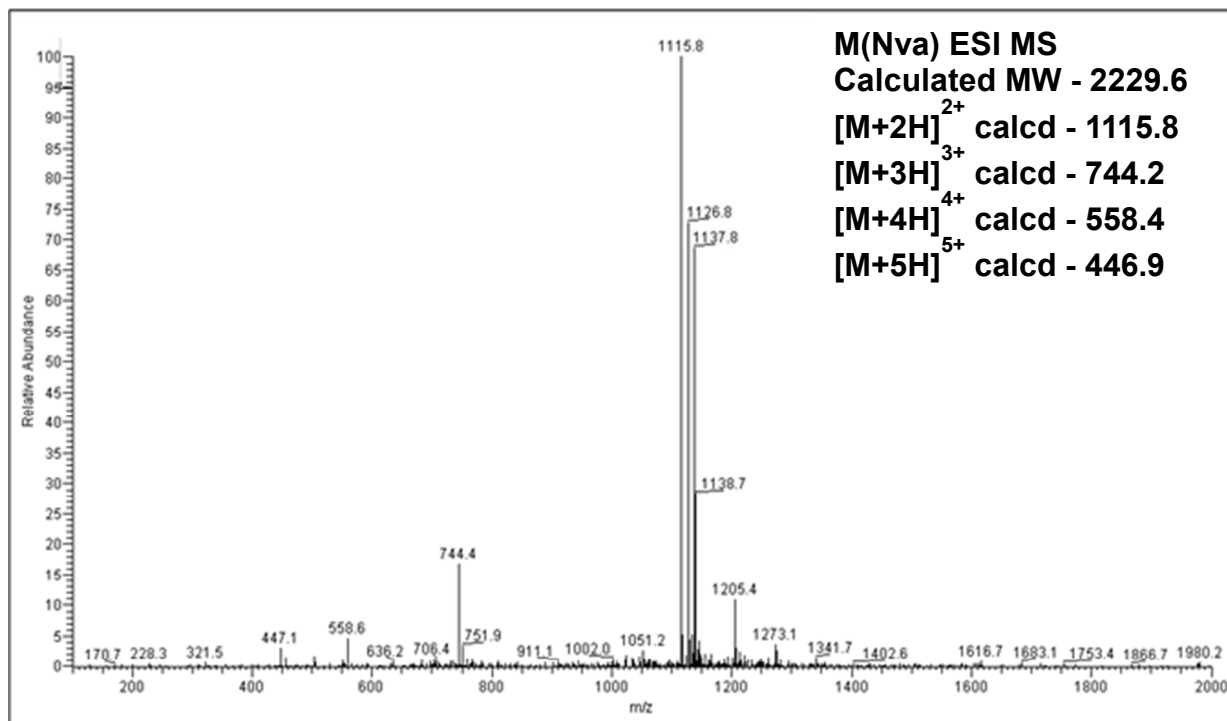
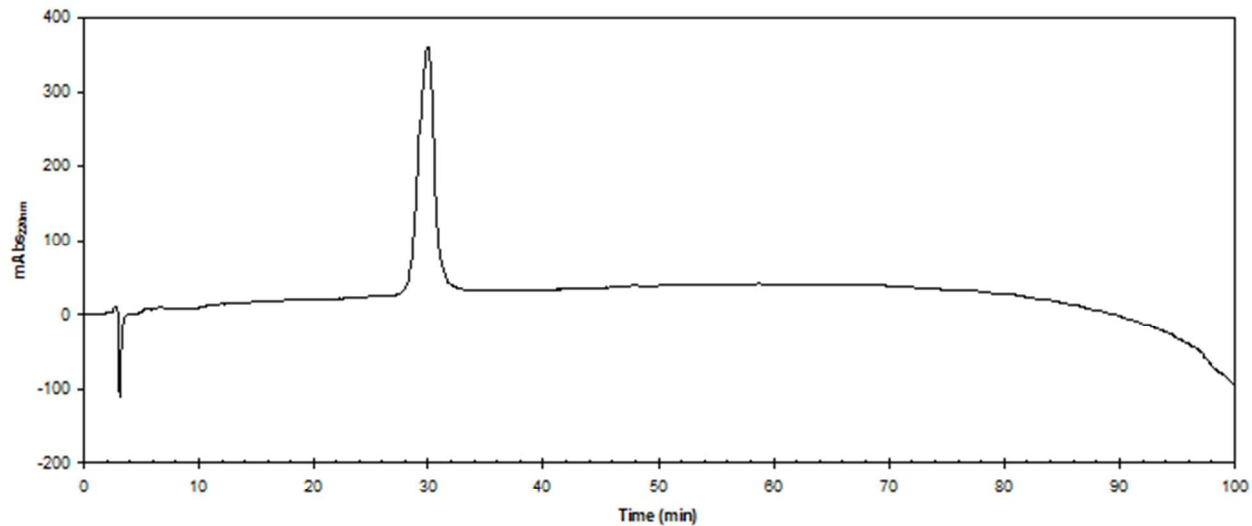


Figure S13: M(Nva) – Analytical HPLC (Vydac C18) 0-100% B; 100 min; 20°C.

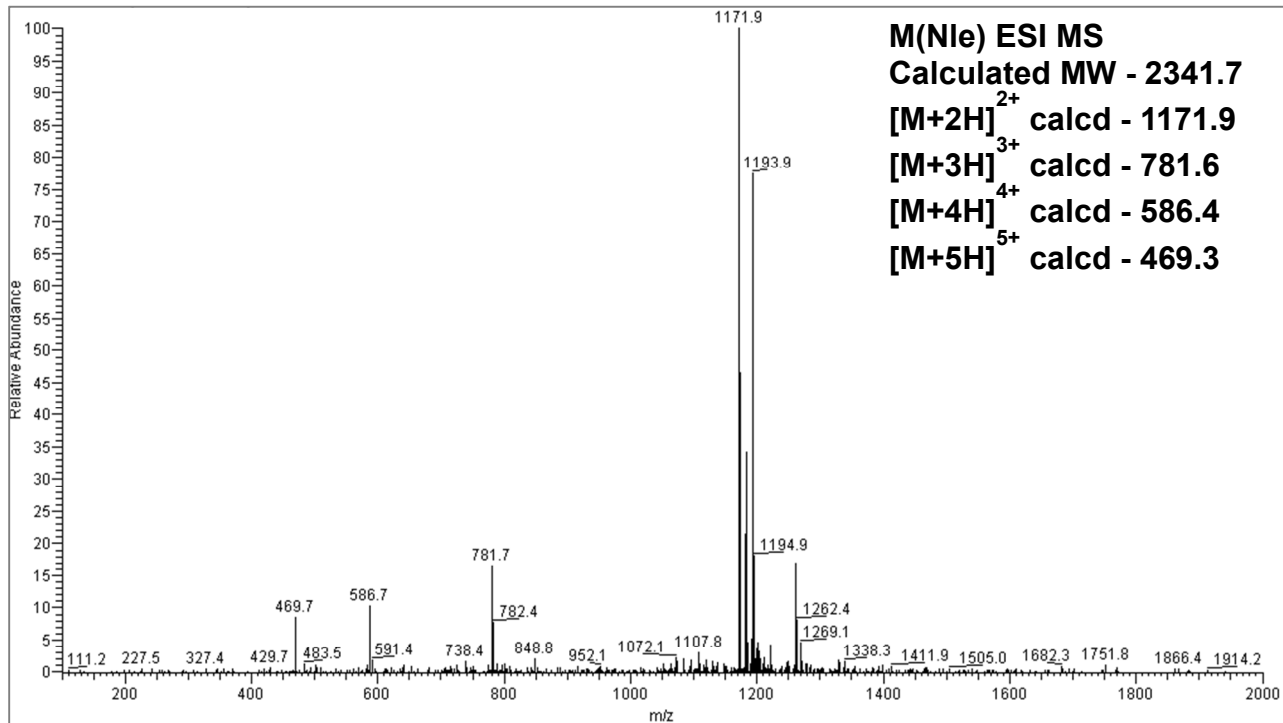
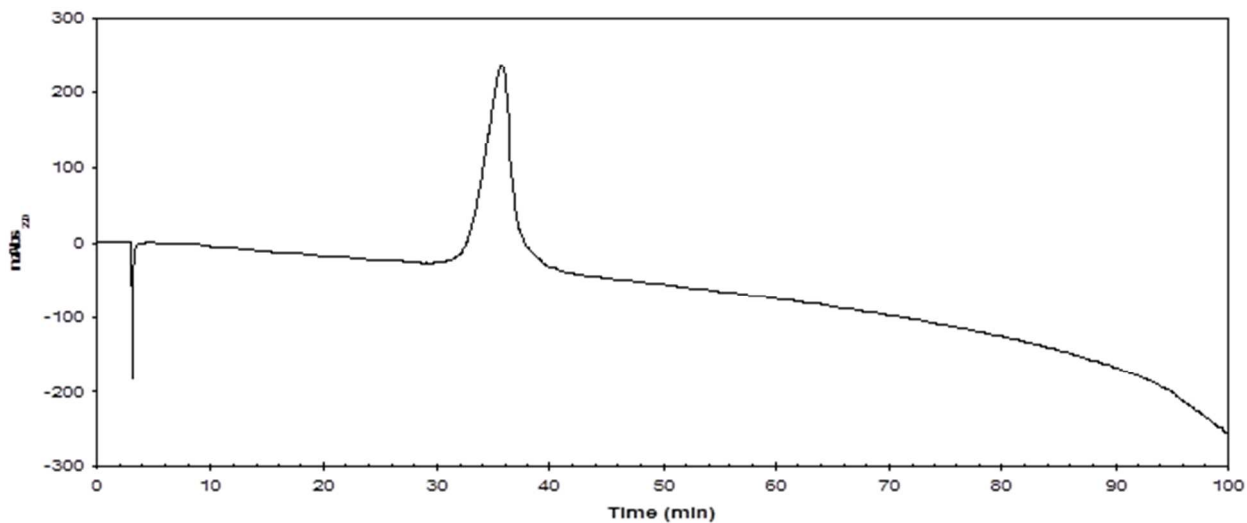


Figure S14: M(Nle) – Analytical HPLC (Vydac C18) 0-100% B; 100 min; 20°C.

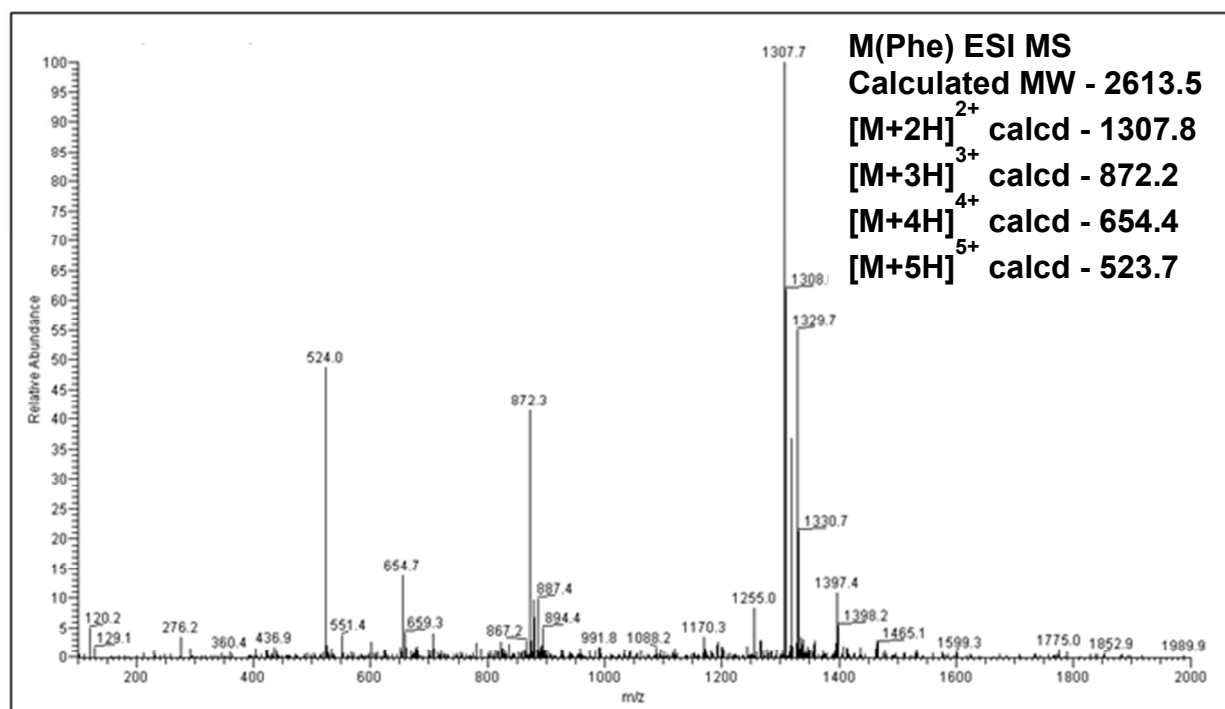
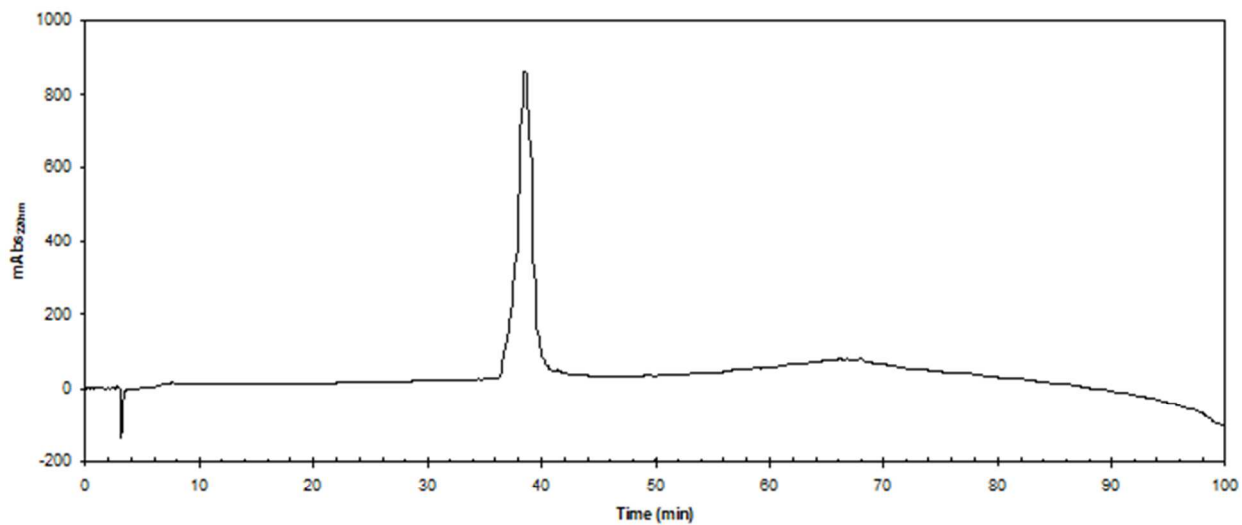


Figure S15: M(Phe) – Analytical HPLC (Vydac C18) 0-100% B; 100 min; 20°C.

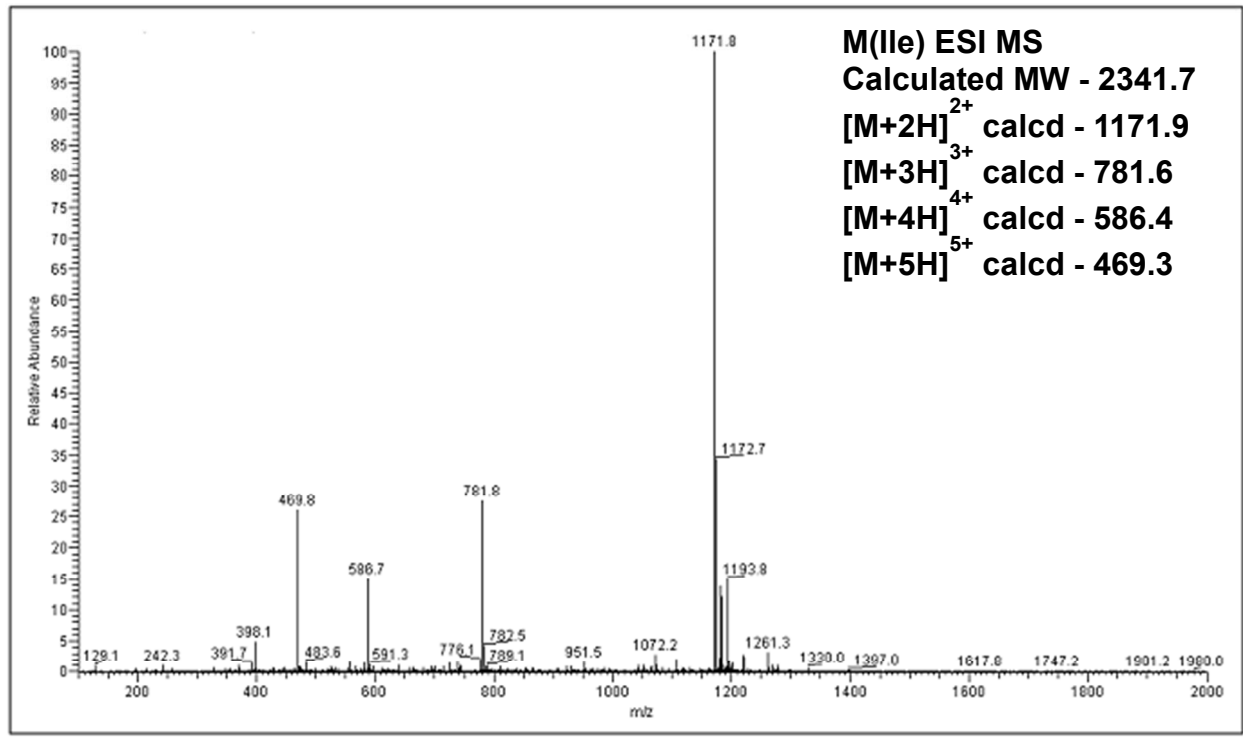
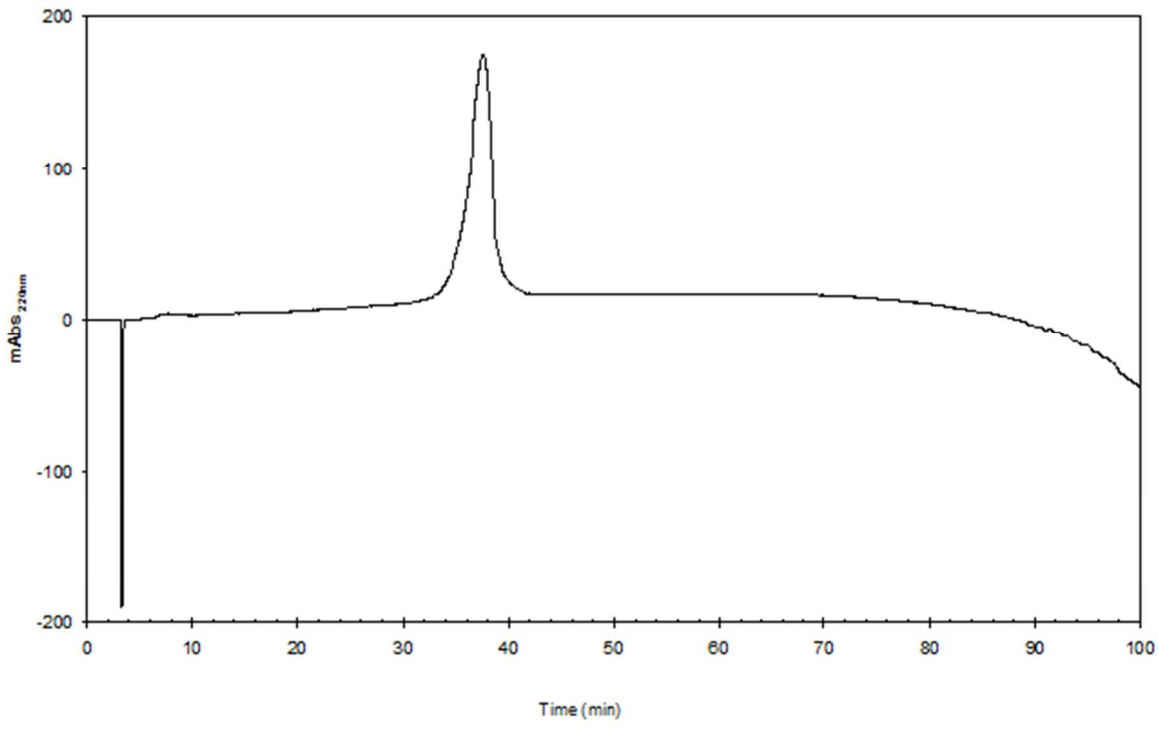


Figure S16: M(Ile) – Analytical HPLC (Vydac C18) 0-100% B; 100 min; 20°C.